Monatshefte für Chemie - Chemical Monthly (2021) 152:151–165
https://doi.org/10.1007/s00706-020-02726-y

ORIGINAL PAPER

Radical-induced cationic frontal polymerisation for prepreg technology

Anh Dung Tran[1] · Thomas Koch[2] · Robert Liska[1] · Patrick Knaack[1]

Received: 26 November 2020 / Accepted: 19 December 2020 / Published online: 23 January 2021
© The Author(s) 2021

Abstract

In this study, a new type of prepreg technology has been established using a dual curing system consisting of 1,6-hexanediol diacrylate (HDDA) and frontally polymerisable components based on the epoxide resin. The study of the polymerisation of HDDA revealed (*tert*-butylcyclohexyl)peroxydicarbonate (BCPC) as the most suitable radical thermal initiator. The presence of BCPC resulted in a fast radical polymerisation of HDDA and no cationic ring-opening reaction of the epoxy, which was observed by monitoring the double bond and epoxy group conversion in real time-NIR rheology measurement. The formed prepreg can subsequently be cured by radical-induced cationic frontal polymerisation of the epoxy resin. Effects of HDDA amount on the radical polymerisation, stiffness of the gel, frontal parameters and thermal mechanical properties of final polymers were investigated. With 10 wt% HDDA, the formed prepreg has very good storage stability, which was proved by monitoring the epoxy group conversion during 4 months of storage at 50 °C while still a stable front can be obtained. Furthermore, the RICFP-prepregs with different fibre contents were prepared and polymerised by RICFP. Then, a snowflake composite was successfully produced using RICFP-prepreg.

Graphic abstract

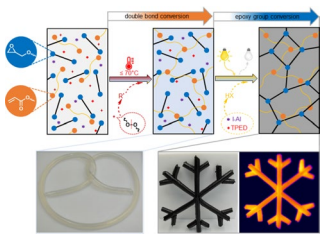

Keywords Polymerisations · Gels · Prepreg · Dual curing · Epoxy resins · Acrylates

Introduction

Prepregs are semi-finished products consisting of fibres pre-impregnated with a thermoplastic or thermosetting resin [1–3]. As an important matrix in fibre reinforced composites, epoxy resins are the most commonly used to produce prepregs [2, 4]. For manufacturing, the fibres are firstly impregnated with a low viscosity resin formulation. Afterwards, the resin is only partially cured to reach a viscous stage (so called B-stage) which prevents the resin flowing out of the fibres during storage and handling [1]. Because of their advantages in ready-to-use materials and outstanding properties of final products, epoxy-based prepregs are

Supplementary Information The online version contains supplementary material available at https://doi.org/10.1007/s00706-020-02726-y.

✉ Patrick Knaack
patrick.knaack@tuwien.ac.at

[1] Institute of Applied Synthetic Chemistry, TU Wien, Getreidemarkt 9/E163-MC, 1060 Vienna, Austria

[2] Institute of Materials Science and Technology, TU Wien, Getreidemarkt 9/E308, 1060 Vienna, Austria

widely used in many applications, such as wind turbines [5–7], sports equipment [8], automotive [9, 10], aerospace [11–13], etc. Commonly, formulations for fibre pre-impregnation are based on components for thermally cured resins, with a hardener and accelerator if needed. Owing to the limited pot-life of these formulations, it is difficult to control the curing reaction at the so-called B-stage, which results in a very poor storage stability of the prepregs [1, 4]. In order to increase the stability, prepregs are normally stored at low temperatures e.g. − 18 °C right after their manufacturing [1, 14, 15]. There are also types that can be stored at room temperature, but they have to be cured then at even higher temperatures due to the lower reactivity of the resin formulations [4, 16–20].

Frontal polymerisation is a fast and energy-efficient process in which a localised polymerisation zone is initiated and moves through the whole monomer formulation [21–27]. Recently, a process called radical-induced cationic frontal polymerisation (RICFP) has been developed for bubble-free bulk curing of epoxy resins [28–32]. In RICFP, a three main component formulation consisting of an epoxy resin, a radical thermal initiator and a photoacid generator can be initiated thermally or under UV light irradiation. In the case of light initiation, the photoacid generator is decomposed and forms a super acid which starts cationic ring-opening polymerisation of the epoxy. The ring-opening reaction releases exothermic heat and then dissociates the radical thermal initiator to form radicals. Afterwards, these radicals interact with the photoacid generator in a redox reaction to liberate again the super acid and therefore keep the polymerisation spreading through the whole formulation without necessity of further irradiation [32]. With the presence of the radical thermal initiator, RICFP can also be initiated by external heat if it is higher than onset temperature of the polymerisation around 100 °C [33]. The previous works indicated that RICFP is not only a fast and energy-efficient process, but also the formulations have a long pot-life if stored in the dark [31, 33]. Furthermore, RICFP was successfully applied to produce epoxy-based composites with different types of fillers and fibres [28–30, 34]. The composites with high content of fillers and good mechanical properties were produced within minutes by RICFP instead of hours thermal curing. With these advantages, in combination with the idea of having long pot-life formulations, a new type prepreg so called "RICFP-prepreg" should be established, which benefits in good storage stability, ready-to-use material and frontal polymerisability.

Our approach to prepare RICFP-prepregs is based on the classic prepreg manufacturing process. A low viscosity formulation is used to impregnate the fibres. Then, the formulation is pre-cured to form a highly viscous or sticky gel (B-stage). RICFP-prepregs should be storable at room temperature for several weeks to months without further curing as long as they are kept in the dark. In order to do this, a radically polymerisable monomer can be used in a mixture with a RICFP formulation. After impregnation of the fibres, the formulation is radically polymerised to form the B-stage. Later, RICFP is applied on demand to fully cure the epoxy monomers. For this approach, acrylates can be used as the radically polymerisable monomers. Depending on types of the radical initiator, the polymerisation of acrylates can be done by thermal or photo-curing [35, 36]. Studies of a system consisting of acrylates and epoxy monomers were presented in different publications [37–40]. These works investigated interpenetrating networks which were formed via simultaneous polymerisation of the two monomers or sequential curing process. However, in preparation of RICFP-prepreg, the challenge is that the radical polymerisation process and the cationic ring-opening reaction needs to be separated. Furthermore, the radical initiators and polymerisation of acrylates should not affect the radical-induced cationic frontal polymerisation of the epoxy-based system.

In this study, a matrix formulation for preparation of RICFP-prepreg was investigated with 1,6-hexanediol diacrylate (HDDA) as a radically polymerisable monomer in a mixture with a frontal formulation based on epoxy resins. To form the B-stage, the radical polymerisation of acrylates was studied with different radical thermal initiators. A formulation consisting of BADGE as epoxy resin, (3-ethyloxetan-3-yl)methanol (EOM) as reactive diluent, 1,1,2,2-tetraphenylethane-1,2-diol (TPED) as radical thermal initiator and bis(4-*tert*-butylphenyl)iodonium tetrakis(perfluoro-*tert*-butyloxy)aluminate (I-Al) as photoacid generator was used for the radical-induced cationic frontal polymerisation. Gelation process was investigated for formulations with different weight ratios of acrylate and frontally polymerisable portions. Double bond and epoxy group conversion were followed using a real time near infrared spectroscopy during rheology measurement. Effects of acrylate portion on the frontal parameters, epoxy group conversion and thermal mechanical properties of the final polymers were also studied. As a crucial parameter in prepregs, storage stability of the gel was investigated. Furthermore, RICFP-prepregs were prepared with different contents of carbon fibre tow. Finally, for proof of concept, a snowflake structure, which should show the spread of the frontal polymerisation, was assembled from many prepreg segments and polymerised by RICFP.

Results and discussion

Study of radical thermal initiators for polymerisation of the acrylate monomer

The aim of this study is to prepare a highly viscous or gelled B-stage which can be polymerised on demand by RICFP. Ideally, the gel should be formed by radical polymerisation of acrylates in a two-monomer formulation. Then, with the presence of the second cationic epoxide monomer formulation, the gel is polymerised by RICFP to form the final polymer. For this dual curing system, two radical thermal initiators are needed in the formulations. The first radical thermal initiator is used for the polymerisation of the acrylates while not effecting the RICFP system. The second is 1,1,2,2-tetraphenyl-1,2-ethandiol (TPED) for the radical-induced cationic frontal polymerisation of the epoxide. The radical thermal initiator (RTI) for the polymerisation of acrylate monomers needs to meet requirements. Firstly, it should have decomposition and polymerisation temperatures lower than the onset temperature of the frontal polymerisation, otherwise the cationic reaction of the epoxy monomer will start. The temperature for the polymerisation of the acrylate should not be higher than 70 °C. Secondly, during the polymerisation of the acrylates these radicals formed from the initiator should not undergo a redox reaction with the photoacid generators (PAGs) to form a super acid for cationic polymerisation of the epoxy monomers.

To find suitable radical thermal initiators (RTIs) for polymerisation of the acrylates, formulations were prepared with 1,6-hexanediol diacrylate (HDDA) and 2 mol% of different radical initiators (AIBN, ACVA, BCPC, PODIC, KPS in Fig. 1). DSC measurements with a heating rate of 5 °C min^{-1} were performed for all these formulations. DSC plots from the measurements give information about the polymerisation temperature (onset temperature) and how fast the polymerisation occurs.

Figure 2 shows exothermic plots of the formulations containing HDDA (1,6-hexanediol diacrylate) with 2 mol% of different radical thermal initiators. Information of the onset temperature and heat of the polymerisation are shown in Table S3 (Supporting information). It can be seen that the

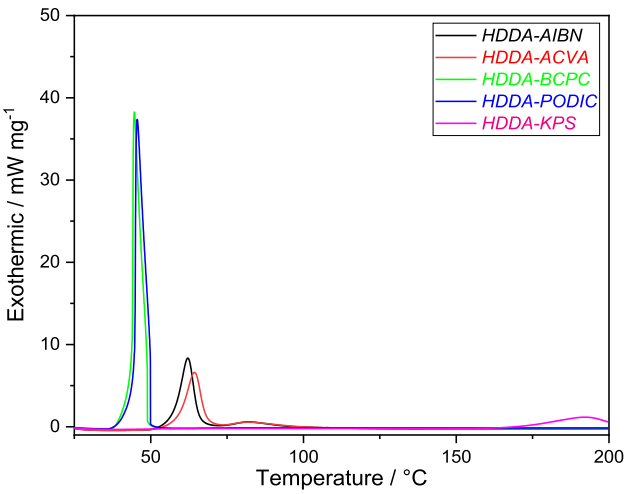

Fig. 2 DSC plots of formulations consisting of HDDA and 2 mol% of different radical thermal initiators

Fig. 1 Acrylate monomer and different radical thermal initiators with their 10 h half-life temperature ($T_{1/2,\,10\,h}$) [41, 42]

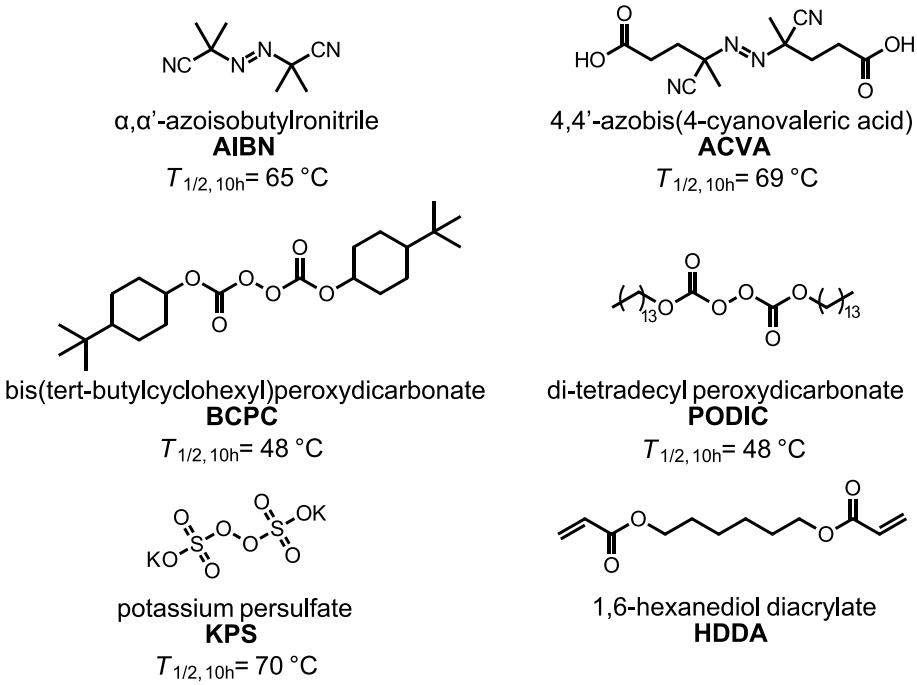

polymerisation of the formulations (except KPS) occurs at temperatures which are lower than 70 °C. The formulations containing BCPC and PODIC are reacted at around 45 °C which is lower than those of formulations with AIBN and ACVA (around 57 °C). The high and sharp exothermal peaks also indicate that the polymerisation obtained from the formulations containing BCPC and PODIC are faster, as compared to the other two formulations.

In addition, solubility of the initiators in HDDA was roughly checked by observing dissolution speed of the powders in the monomer. The observation indicates that BCPC and AIBN were easy and fast to dissolve in the monomer, while PODIC and ACVA were not. The PODIC based formulation was cloudy, while ACVA was precipitated from the solutions in about 10 min after mixing. In case of KPS, no dispersion could be observed. The precipitation occurred immediately after mixing. This explains the missing reaction peak on the DSC plot of the formulation containing KPS.

The above study indicates that BCPC seems to be the most suitable radical thermal initiator for the polymerisation of HDDA. In order to investigate the behaviour of BCPC in a system consisting of radical-induced cationic frontal polymerisable components (Fig. 3), an acrylate-epoxy formulation was prepared with 20 wt% radically polymerisable portion and 80 wt% frontally polymerisable portion. Composition of the radical polymerisable portion was the same as the formulation *HDDA-BCPC* which includes 2 mol% (3.5 wt%) of BCPC in HDDA. The frontal polymerisation formulation (called *FP*) was prepared with BADGE and EOM ((3-ethyloxetan-3-yl)methanol) (with a molar ratio of 100:40, respectively), 2 mol% (2.5 wt%) TPED and 1 mol% (4.6 wt%) I-Al. Then, the acrylate-epoxy formulation is abbreviated to *FP_20HDDA-BCPC*. To observe the radical polymerisation of this formulation, DSC measurement was conducted in a temperature range of 25–200 °C, with a heating rate of 1 °C min^{-1}. The same measurements were done for three other formulations to confirm the polymerisation of two systems. The first one was the neat frontal formulation (*FP*). The others were based on the formulation *FP_20HDDA-BCPC*, but without BCPC (*FP_20HDDA*) and one without HDDA (*FP_BCPC*).

The DSC plots of these formulations are shown in Fig. 4. It can be seen that the radical-induced cationic frontal polymerisation of *FP* rapidly occurs with a high and sharp exothermic peak at the temperature higher than 80 °C. In comparison with *FP,* the presence of BCPC in the formulation *FP_BCPC* results in a reaction at lower temperature, which means that the radicals formed from BCPC can undergo a redox reaction with the photoacid generator to liberate a super acid for the cationic ring-opening of the epoxide. The exothermic peak of *FP_BCPC* is wider and lower than those of *FP*, which could be since the radicals from BCPC are less effective in the redox reaction with the photoacid generator than those from TPED. This statement was confirmed by

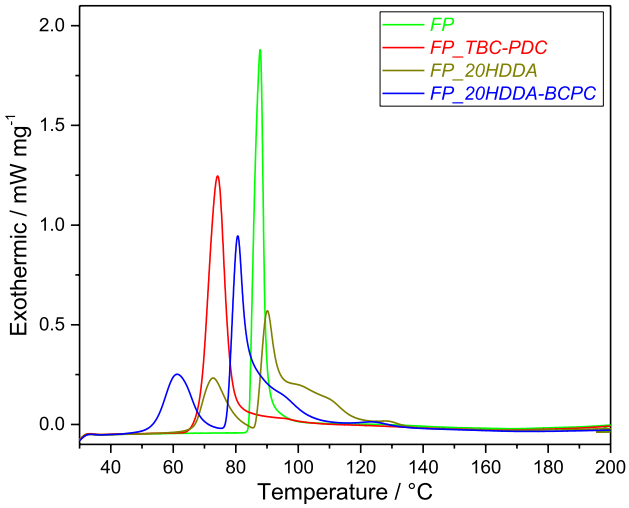

Fig. 4 DSC plots of the formulations *FP*, *FP_BCPC*, *FP_20HDDA* and *FP_20HDDA-BCPC*

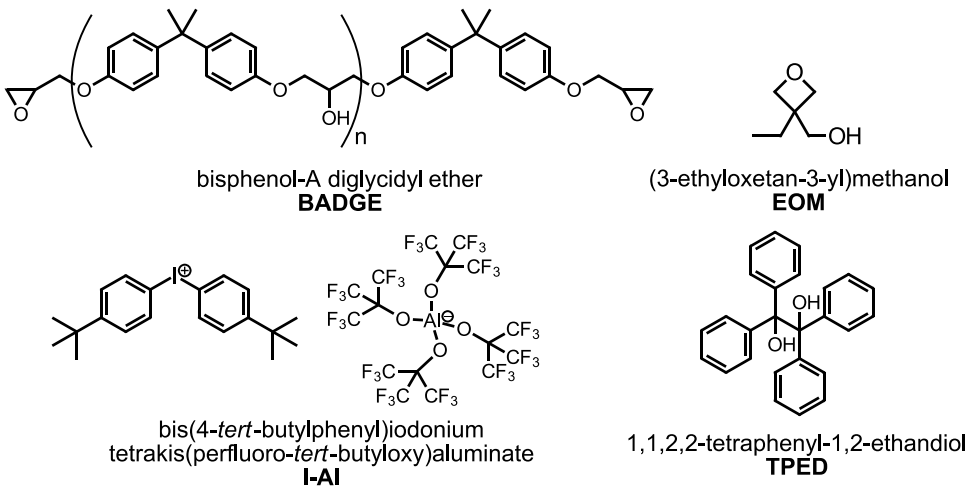

Fig. 3 Chemical structure of components in the frontal formulation (*FP*)

DSC measurements of two frontal formulations containing 2 mol% of different radical thermal initiators (TPED and BCPC, Fig. S5, supporting information). With the use of BCPC, even though the cationic ring-opening reaction occurred at lower temperature, the exothermic peak of this formulation is broader and lower than those of the *FP* with *TPED* (Fig. S5, Supporting information). In cases of the formulations containing HDDA, there are two separated exothermic peaks during the measurements. The first one is the radical polymerisation of HDDA, while the second is the cationic ring-opening polymerisation. In *FP_20HDDA*, the radical polymerisation is observed at around 70 °C, which was initiated by the radicals cleaved from TPED molecules. The polymerisation peak at around 70 °C of formulation containing only HDDA and TPED as radical thermal initiator is shown in Fig. S6 (Supporting information). In case of *FP_20HDDA-BCPC*, the radicals formed from BCPC result in the polymerisation of HDDA at lower temperature. A shoulder at the second peak in these two measurements might be due to effect of polyacrylates on the ring-opening polymerisation of the cationic monomers. The most important information from these measurements is the radical polymerisation and the cationic ring-opening reaction did not take place at the same time. In all the cases, the radical polymerisation always finished before starting the cationic reaction.

To deeply investigate effects of BCPC on the radical polymerisation and cationic ring-opening reaction, real time (RT)-NIR rheology measurements were conducted for these four formulations introduced above. The rheology measurements were conducted at 70 °C for at least 60 min. During the measurements, NIR spectra were recorded every 3 min to follow the double bond and epoxy group conversion.

Figure 5 shows the rheology data of the four formulations. It can be seen that the storage and loss moduli of *FP* containing only the frontal formulation are stable during the whole measurement. This means that the ring-opening reaction of the cationic monomers did not take place during the measurement at 70 °C. With *FP_BCPC* containing the frontal formulation and BCPC, the storage modulus curve crossovers the loss modulus at a gel time, t_{gel}, of about 30 min. The result indicates that radicals liberating from the decomposition of BCPC interact with the photoacid generator I-Al to promote the cationic ring-opening polymerisation. In comparison with *FP_BCPC*, the formulation containing HDDA (*FP_20HDDA-BCPC*) has a shorter gel time of about 16 min, while the maximum storage modulus is lower. This illustrates that the formed radicals selectively attack the double bonds to radically polymerise HDDA and no cationic ring-opening reaction occurs. This assumption can be confirmed by the NIR measurements below. Furthermore, the storage and loss moduli of the formulation *FP_20HDDA* without BCPC slowly increase after 80 min,

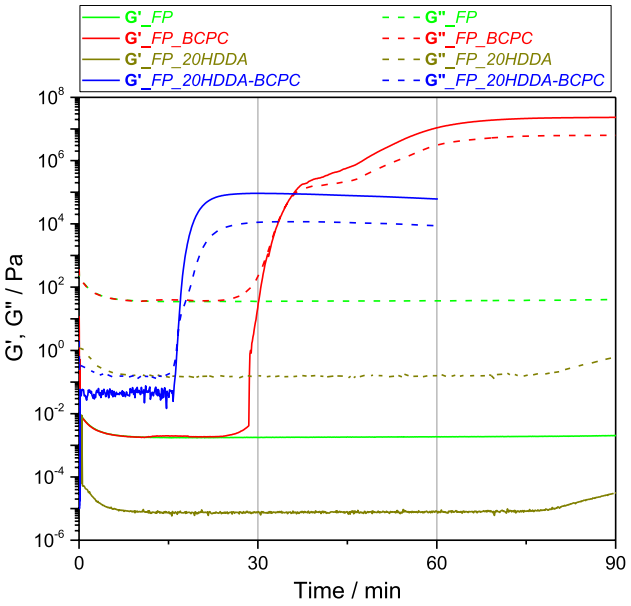

Fig. 5 Rheology measurements at 70 °C of the formulations *FP*, *FP_BCPC*, *FP_20HDDA* and *FP_20HDDA-BCPC*

which attributes to the polymerisation of HDDA caused by the radicals from TPED. This is in an agreement with the DSC study above.

NIR spectra measured after 0, 15, 30 and 60 min at 70 °C of the formulation containing 20 wt% HDDA (*FP_20HDDA-BCPC)* are shown in Fig. S7 (Supporting information). In the NIR spectra, peaks at 4530 cm^{-1} and 4620 cm^{-1} are the epoxy and phenyl signals, respectively [43, 44]. The peaks at 4483, 4740 and 6160 cm^{-1} are assigned to the double bonds of HDDA [43, 45, 46]. In addition, a decrease in the intensity of these double bond signals during the radical polymerisation can be seen in Fig. S8 (Supporting information), showing NIR spectra of the formulation containing only HDDA and 2 mol% BCPC measured at 50 °C (around polymerisation temperature in Fig. 2) after 0, 5 and 10 min.

During the RT-NIR rheology measurement, the signals at 4530 and 6160 cm^{-1} were chosen to follow the epoxy group and double bond conversion, respectively. The conversion was calculated by decrease of the integral of the functional groups referenced to the integral of the phenyl signal at 4620 cm^{-1} which does not change during the measurement. Owing to the overlap of the double bond signal at 4483 cm^{-1} and epoxy ring at 4530 cm^{-1}, separation of these peaks was done using a peak deconvolution function in OriginPro 2020 SR1 9.7.0.188. Afterwards, area of the signals at 4530 cm^{-1} (epoxy ring), 6160 cm^{-1} (double bond) and 4620 cm^{-1} (phenyl as a reference) was integrated using the same software to calculate the functional group conversion.

In Fig. 6, the round-marker plots (green and dark yellow) corresponding to the epoxy group conversion stably remain

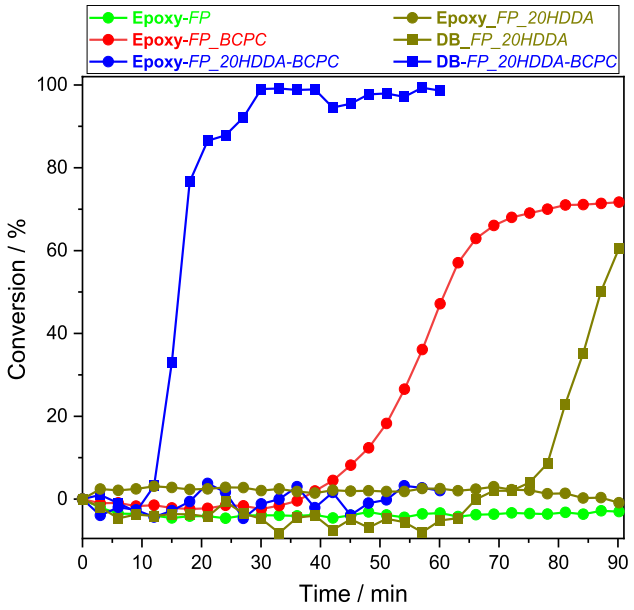

Fig. 6 The epoxy group and double bond conversion of the formulations *FP*, *FP_BCPC*, *FP_20HDDA* and *FP_20HDDA-BCPC*

at around zero percent conversion, which indicate that the cationic ring-opening reaction of the epoxides did not occur during the measurement of *FP* and *FP_20HDDA* formulations containing no BCPC. In *FP_BCPC*, the radicals formed from BCPC interact with the PAG liberating a super acid to start the cationic polymerisation of the epoxides. Here, at 70 °C, the epoxy group conversion starts to increase slowly after 30 min and reaches about 70% after 90 min. With the full formulation *FP_20HDDA-BCPC*, the radicals from BCPC selectively attack the double bonds with high electron density to start the polymerisation of HDDA, which results in a significant increase in the double bond conversion after 10 min. After 30 min, the double bond conversion reaches values of more than 90% and nearly full conversion after 60 min. Moreover, the epoxy group conversion of this formulation is 0% all the time, which means the cationic ring-opening polymerisation did not take places. This confirms that the radicals formed from BCPC prefer attacking the double bonds to undergo the radical polymerisation than reacting with the photoacid generator to form the super acid for the cationic polymerisation.

Therefore, it can be stated that BCPC is the most suitable initiator for this study. The radicals can react with the PAG and therefore start the cationic ring-opening of the epoxides at high temperatures. However, in the presence of radically polymerisable monomers like acrylates, the radicals selectively attack the double bonds and undergo the radical polymerisation. Furthermore, also the radicals formed during the homopolymerisation of HDDA do not decompose the cationic photoinitiator.

Table 1 Summary of the RT-NIR rheology study of formulations containing various amounts of HDDA

Formulation	t_s /min	t_{gel} /min	DBC_{60} /%	G'_{60} /Pa
FP_5HDDA-BCPC	60.2 ± 0.1	–	56.8 ± 2.9	0.1 ± 0.0
FP_10HDDA-BCPC	24.5 ± 0.4	32.1 ± 0.0	98.3 ± 1.7	1022 ± 323
FP_15HDDA-BCPC	17.5 ± 0.9	20.8 ± 0.9	99.0 ± 0.8	30,750 ± 8040
FP_20HDDA-BCPC	16.1 ± 0.6	17.5 ± 1.3	98.2 ± 0.2	58,260 ± 3820

Effects of amount of acrylates on the gelation process

In this study, formulations for preparation of the gels were prepared with different weight percentages (wt%) of the acrylate portion. Ratios of the frontal portion (*FP*) to the acrylate portion (*HDDA-BCPC*) were 95:5, 90:10, 85:15, 80:20 in wt%, respectively. Both components of these formulations contain the given fixed amount of initiators shown in the previous chapter. All the formulations were purged with argon for 5 min and then immersed in an ultrasound bath (with cool water) for 10 min to remove dissolved oxygen and bubbles.

First, the RT-NIR rheology measurement was conducted for all the formulations. The rheology data and the conversion of double bonds and epoxy groups for all the formulations are shown in Figs. S9 and S10 (Supporting information). In accordance to the above discussed results, only the radical polymerisation took place during the whole measurements. This can be seen by an increase in the double bond conversion, while the epoxy group conversion is around zero. Table 1 presents a summary of measurements data. In addition to the gel time (t_{gel}), t_s is the time when the radical polymerisation starts and the storage modulus starts to increase. DBC_{60} and G'_{60} are the double bond conversion and the storage modulus at 60 min of the measurement, respectively.

These results indicate that the formulation containing 5 wt% HDDA portion has very slow radical polymerisation and does not have a gel point due to the too low amount of acrylates. With an increase of HDDA amount, it is obvious that the gelation time decreases. In addition, time gaps between t_{gel} and t_s decrease with the increase in HDDA amount, which means that the rate of the radical polymerisation increases. The results also reveal that the double bond conversion at 60 min, DBC_{60}, is close to 100% in the formulations consisting of 10 wt% HDDA or higher. Furthermore, the storage modulus value at the end of the measurement gives information about stiffness of the gels. In Table 1, G'_{60} of the formulation *FP_5HDDA-BCPC* is

very low and the specimen was still liquid. This value is around 1000 Pa for the formulation *FP_10HDDA-BCPC* which results in a flexible gel. The flexibility of this gel can be seen in Fig. S11 and Video 1 (Supporting information), where it was used to make a "bretzel" form cured by RICFP. With an increase of HDDA amount, the storage modulus value at 60 min significantly increases, which is owned to an increase of crosslink density. With 20 wt% of HDDA portion, G'_{60} of the gel is about 50 times higher than the value of *FP_10HDDA-BCPC*. Owing to the increase in the gel stiffness to impractical heights, formulations containing more than 20 wt% HDDA were not being considered.

Additional to the RT-NIR measurement, all the formulations were transferred to 1 cm^3 syringes. Then, the gelation process or the radical polymerisation of HDDA was done by immersing the syringes in a water bath at 60 °C for 90 min. In this experiment, the temperature for the radical polymerisation was set to 60 °C instead of 70 °C in the RT-NIR rheology measurement to prevent localised over heating which might lead to the frontal polymerisation of the cationic monomers. The gels were then collected and the NIR spectra were measured to check the double bond conversion (DBC). Gel content was also determined by extracting the specimen with dichloromethane.

Table 2 illustrates the gel content and double bond conversion of the four specimens. It can be seen that double bond conversion for all the specimens is very similar to those obtained from the rheology measurements at 70 °C. The gel content of the specimens *FP_10HDDA-BCPC*, *FP_15HDDA-BCPC* and *FP_20HDDA-BCPC* are very close to the initial weight percentages of the acrylate portion. Furthermore, HPLC measurements of dried residues from the extracted solutions were done. The chromatogram of *FP_10HDDA-BCPC* in Fig. S12 (Supporting information) shows no HDDA signal at retention time of about 8 min. This strengthens the statement that a high double bond conversion was obtained and the cationic polymerisation of the epoxy system did not take place during the gelation process. In case of the specimen *FP_5HDDA-BCPC*, the gel content is lower than the initial weight percentage of HDDA portion, which is due to low double bond conversion.

Table 2 Gel content and double bond conversion of the specimens from formulations containing various amounts of HDDA

Gel	HDDA:FP wt%:wt%	DBC/%	Gel content/%
FP_5HDDA-BCPC	05:95	67.7 ± 7.2	1.50 ± 0.34
FP_10HDDA-BCPC	10:90	97.0 ± 0.0	9.92 ± 0.17
FP_15HDDA-BCPC	15:85	97.2 ± 0.5	15.21 ± 0.37
FP_20HDDA-BCPC	20:80	98.3 ± 1.1	21.05 ± 0.29

Furthermore, the specimens (except *FP_5HDDA-BCPC*) remained after the extraction with similar shapes, but in smaller sizes. This reveals that a homogeneous network of polyacrylates was formed in these gels and was not collapsed during the extraction with the solvent. Moreover, the gel containing 10 wt% acrylate (*FP_10HDDA-BCPC*) was chosen to observe the extraction process under a light microscope. A thin section of about 0.5 mm thickness was put on a small petri dish which was placed under the light microscope attached with a camera. Figure 7 illustrates light microscopic images of the gel. The top and middle images are the gel before immersing in dichloromethane, which indicate a bubble-free surface. The bottom image was taken at 4 min after adding the solvent, a flow of bubbles was formed in the gel due to diffusion of dichloromethane and the extraction process. First, the solvent diffused into the section and

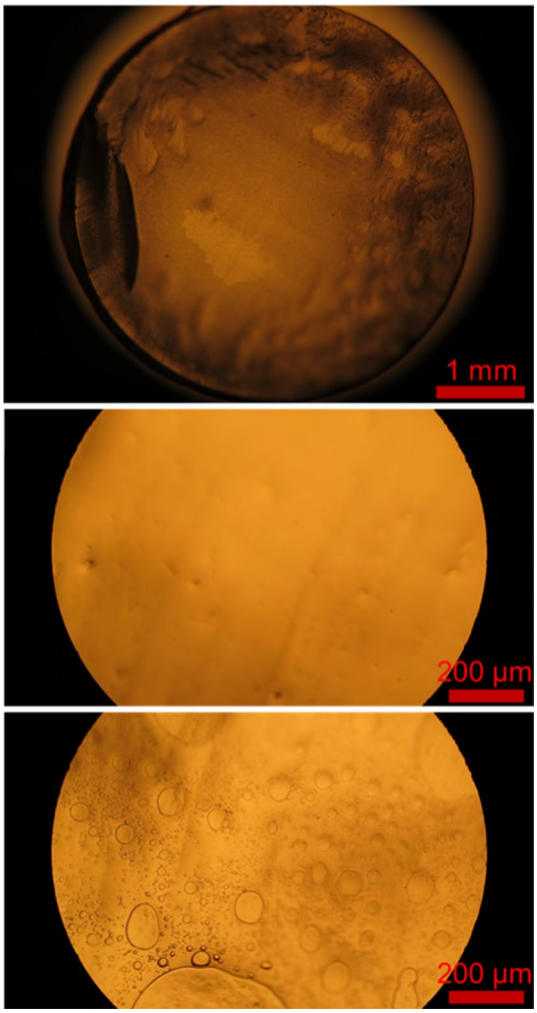

Fig. 7 Light microscopy images of the gel *FP_10HDDA-BCPC* (top: before adding CH_2Cl_2, 5 times of magnification; middle: before adding CH_2Cl_2, 20 times of magnification; bottom: 4 min after adding CH_2Cl_2, 20 times of magnification)

formed many small bubbles on the whole surface. Then, the extraction occurred and the small bubbles combined to form the bigger bubbles.

Figure 8 shows light microscopic images of the extracted specimen (*FP_10HDDA-BCPC*) after the removal of solvent from the gel content experiment. The top image (taken at 0 s) is the extracted gel after dried in a vacuum oven. It can be seen that the diameter of the specimen is about 3 times smaller than the original gel (Fig. 7, top). To observe swelling process, dichloromethane was added on the specimen. The middle image was taken at 30 s after the addition of the solvent. Owing to the diffusion of the solvent, the specimen was swollen and bubbles were formed. Then, the last image was taken at 40 s after the middle image when almost all of the solvent evaporated. It is clearly seen in the bottom image that the bubbles almost disappeared and the specimen returned to the original shape as similar in the top image. This confirms a homogenous and stable network of polyacrylates in the gel.

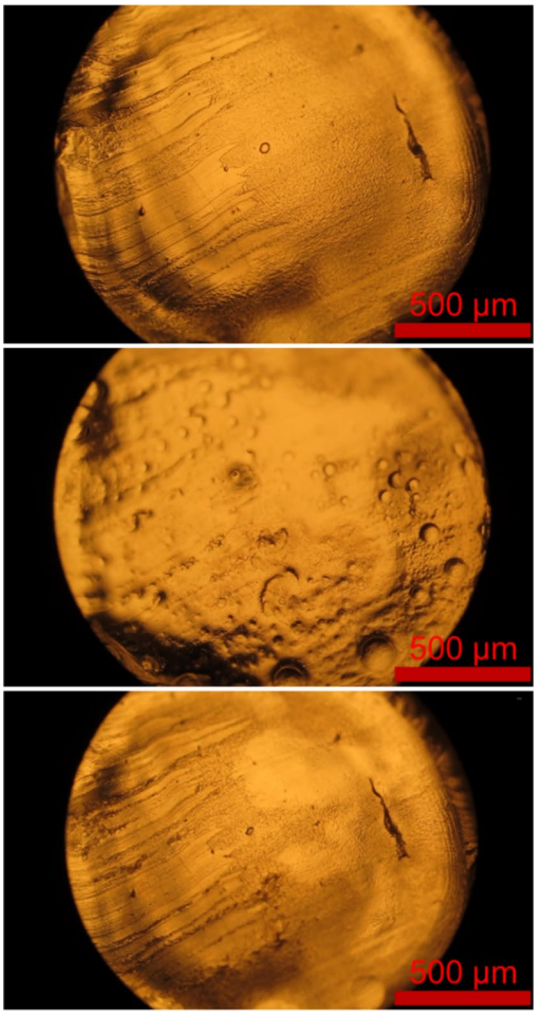

Fig. 8 Light microscopy images of *FP_10HDDA-BCPC* after extracted with CH_2Cl_2 (top: before adding CH_2Cl_2, middle: 30 s in CH_2Cl_2, bottom: when CH_2Cl_2 evaporated)

Storage stability of the formulation and the gel

Stability of the formulation decides a processing time window when the impregnation of the fibres should be carried out before the viscosity of the formulation starts to increase. To test the stability, about 3 g of the formulations were stored at room temperature after the preparation. Following storage time up to 7 days, viscosity and NIR spectra of the formulations were measured at 25 °C. The double bond and epoxy group conversion were calculated from the signal integration in NIR spectra to follow the polymerisation of the monomers.

Figure 9 shows the viscosity and functional group conversion of the formulations containing 10 wt% and 20 wt% HDDA portion. It can be seen that the viscosity, double bond and epoxy group conversion of the two formulations have no significant change. This means that the formulations are stable at room temperature up to 7 days, which is long enough for processing. Furthermore, the RT-NIR rheology measurement at 70 °C was performed for the formulations on day 7th to check the gelation process. The results are shown in Table S4 (Supporting information). The t_s, t_{gel} and DBC_{60} of the formulations on day 7th are close to these values of the fresh formulations.

In addition, storage stability of the gel is an important parameter in the study of prepregs. It decides the time the

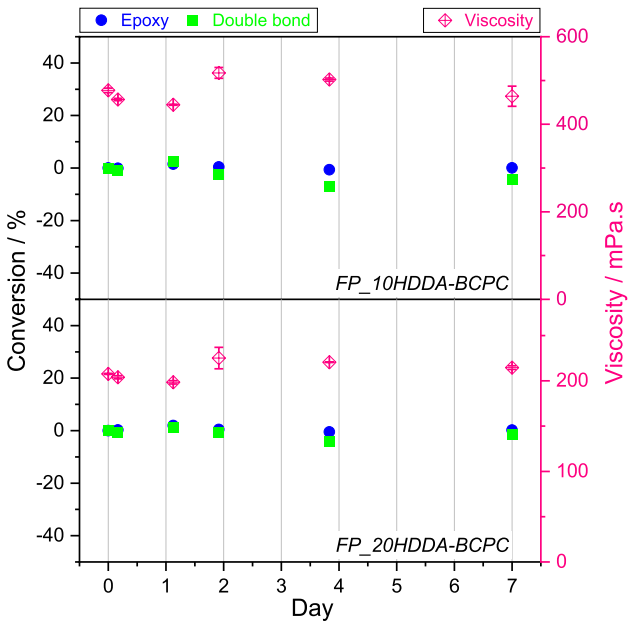

Fig. 9 Viscosity, double bond and epoxy group conversion of the formulations *FP_10HDDA-BCPC* (upper) and *FP_20HDDA-BCPC* (lower) up to the storage of 7 days at room temperature

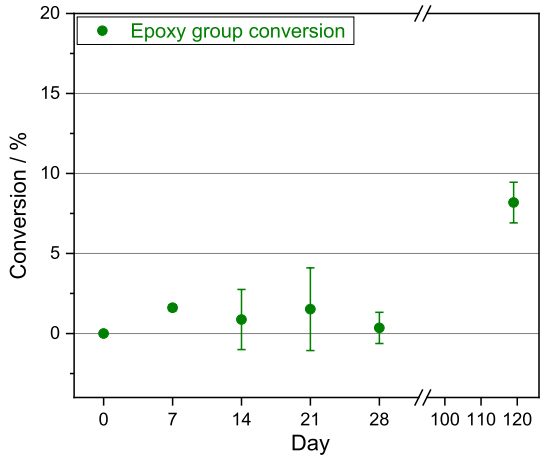

Fig. 10 Epoxy group conversion of the gel *FP_10HDDA-BCPC* measured on different days during storage

prepreg can be stored before usage. For the test, the gel consisting of 10 wt% HDDA was collected in a brown vial and kept in an oven at 50 °C. Following a time schedule, a small piece of the gel was taken and measured the IR spectrum. The epoxy group conversion was calculated using the usual method to check the stability of the gel.

Figure 10 illustrates that the epoxy group conversion remains stable at around 0% up to 1 month. Then, this value slightly increases to about 8% after about 4 months at 50 °C. After 1 and 4 months, the gels were polymerised by RICFP. The frontal velocity and frontal temperature of these experiments are shown in Table S5 (Supporting information). Even after 4 months, a fast and stable front was still observed with a velocity of 4.9 cm min^{-1} as compared to 6.3 cm min^{-1} in RICFP of the fresh gel, while the frontal temperatures were similar.

Radical-induced cationic frontal polymerisation of the gel

In this study, all the gels which were removed from the syringes, were placed on a PTFE mold. The gel was then polymerised by RICFP. The initiation of RICFP was done on one end of the mold with UV/Vis-light of 320 to 500 nm and a light intensity of 3 W cm^{-2} at the tip of the light guide (about 500 mW cm^{-2} on surface of the specimen). After initiation, the reaction propagated without further irradiation being necessary.

For comparison, the two formulations *FP* and *FP_BCPC* were treated in the water bath at 60 °C for 90 min, to mimic the gelation process. *FP* is the frontal formulation, while the composition of *FP_BCPC* is the same as the formulation *FP_20HDDA-BCPC* but without HDDA. After treatment, the formulations were filled in a PTFE mold and polymerised by RICFP with the same initiation and setup as above.

The frontal parameters and epoxy group conversion for all specimens are shown in Table 3. It can be seen that the epoxy group conversion is always higher than 98% for all the specimens. This means that the presence of polyacrylates has no significant effect on the curing degree of the cationic monomers. The frontal velocity and frontal temperature of the *FP* formulation are about 14 cm min^{-1} and 260 °C, respectively. These values are slightly higher in the *FP_BCPC* specimen. This is due to the presence of the additional amount of BCPC. With the specimens containing acrylates, the frontal parameters decrease while the amount of HDDA increases. On the one hand, after the treatment of the formulations at 60 °C, the polyacrylate was formed and dispersed in the gels. The polyacrylate plays a role as a filler. Owing to the heat uptake, while the filler content increases, the frontal velocity and the frontal temperature decrease. On the other hand, the decrease of the cationic monomer fraction results in a reduction of the frontal parameters. The similar behaviour was discussed in our previous work about particle filled epoxy composites [28].

Effects of gelation process on thermal mechanical properties of the final polymers

DMTA measurement of the RICFP specimens was performed in a temperature range of −50 °C to 200 °C with two heating runs. The storage modulus and loss tangent of all the specimens obtained from the first heating run are shown in Fig. 11.

Specimen *FP* has only a T_g peak at around 132 °C. Additional to the T_g at the similar temperature, the specimen *FP_BCPC* which contains an added amount of the initiator BCPC, has a second T_g peak at around − 15 °C. The appearance of the second T_g peak might be due to an inhomogeneous polymer network which caused by a slightly lower epoxy group conversion of this specimen and the thermal treatment process of the formulation. As discussed in the previous chapter, during treatment of the formulation at 60 °C the radicals formed from BCPC interact with the photoacid generator liberating a super acid and starting the cationic

Table 3 Frontal parameters and epoxy group conversion for all specimens

Specimen	V_F /cm min^{-1}	T_F /°C	Epoxy group conversion /%
FP	14.2 ± 0.1	260 ± 11	99.2 ± 1.9
FP_BCPC	16.6 ± 0.0	265 ± 6	98.6 ± 3.8
FP_5HDDA-BCPC	8.1 ± 0.2	241 ± 7	99.4 ± 5.0
FP_10HDDA-BCPC	6.3 ± 0.6	220 ± 2	99.5 ± 2.2
FP_15HDDA-BCPC	4.8 ± 0.1	219 ± 4	99.5 ± 4.3
FP_20HDDA-BCPC	3.2 ± 0.1	195 ± 5	99.5 ± 2.7

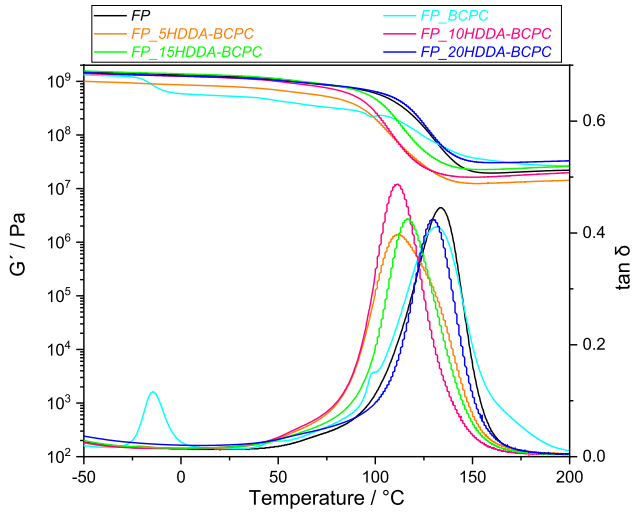

Fig. 11 Storage modulus and tan δ versus temperature obtained from the first heating run

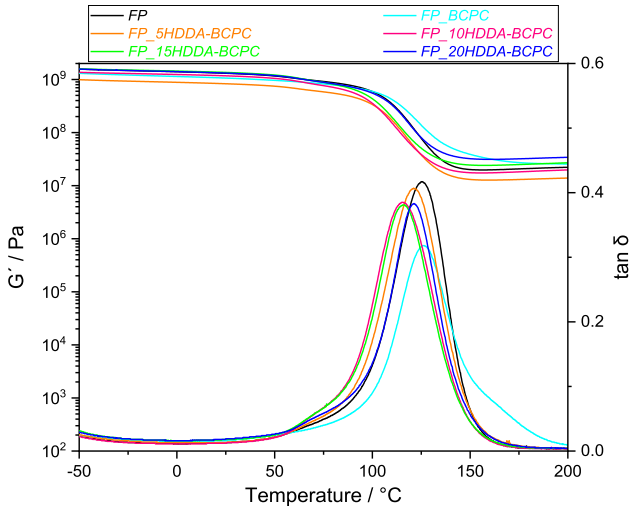

Fig. 12 Storage modulus and tan δ versus temperature obtained from the second heating run

ring-opening of the epoxy monomers. This rather sluggish initiation process might result in formation of oligomers. Even though the frontal polymerisation occurred at high temperature, this very fast curing process might not give enough time for the oligomers to arrange and bond to propagating polymer chains. The oligomers might also affect the epoxy group conversion of this specimen which was slightly lower than other specimens.

In addition, the specimen containing 5 wt% HDDA portion (*FP_5HDDA-BCPC)* has a broad T_g peak which results from an inhomogeneous network of acrylate and epoxy. The low HDDA amount is not enough to form a stable gel in this specimen. In the liquid state, a phase separation of polyacrylate from the epoxy components occurred easily, which results in the inhomogeneous network in the final polymer. With the higher amount of the HDDA, the polymer network becomes more homogeneous which can be seen at the sharp and narrow T_g peaks. In these specimens, a homogeneous dispersion of the polyacrylates in the cationic monomers was confirmed in the gel content experiment and the light microscopic images. The network remains stable in the final polymers.

Figure 12 illustrates the second heating data of the DMTA measurement for all the specimens. It can be seen that in the specimen *FP_BCPC* the T_g peak at low temperature disappeared and only one broad T_g peak is observed. This is due to reorganisation of the inhomogeneous network combining with a post curing in the first heating run at high temperatures. These arrangement and post curing also occurred in the other specimens, which leads to the narrower T_g peaks. The change is most obvious in the specimen *FP_5HDDA-BCPC,* which is clearly seen in a decrease of full width at half maximum of the tan δ peak from 46 to 34 °C (Table S6, Supporting information). In addition, the glass transition temperature slightly decreases with an increase of HDDA amounts from 0 to 15 wt% which correspond to the specimens *FP*, *FP_5HDDA-BCPC*, *FP_10HDDA-BCPC* and *FP_15HDDA-BCPC*, respectively. This results from the decrease of epoxy fraction. Afterwards, with 20 wt% HDDA (*FP_20HDDA-BCPC*) the T_g increases again to a similar value of *FP_5HDDA-BCPC*, which is due to an increase of crosslinking density contributed by polyacrylates.

Preparation of RICFP-prepreg and its composites

In this study, the formulation consisting of 10 wt% HDDA portion and 90 wt% frontal portion (*FP_10HDDA-BCPC*) was chosen to impregnate carbon fibres. The RICFP-prepregs with different fibre contents were produced and then polymerised by RICFP as described in the experimental section.

Figure 13 shows the frontal velocity and frontal temperature of the prepreg specimens. It can be seen that the frontal temperature for all the specimens is similar, while the frontal velocity is slightly faster in the case of composites. Normally, the frontal velocity decreases with an increase of filler content, which was discussed in the previous works [28]. However, if the specimens contain thermally conductive elements and they align along the propagated path of the front, the frontal velocity could be faster than those of the matrix [47, 48]. This is also applicable in this experiment where the thermally conductive carbon fibre tow results in the faster frontal velocity. With the fibre content higher than 40 wt%, the prepreg was collapsed during the removal out of the glass tube. This might be due to the amount of the

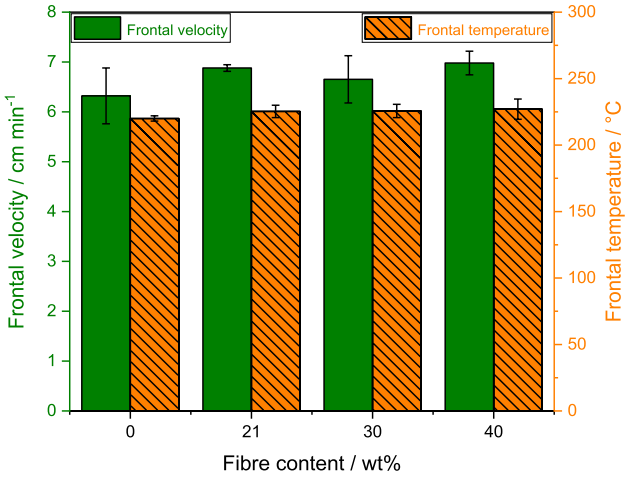

Fig. 13 Frontal parameters of the prepregs with different fibre contents

liquid formulation, which was not enough to form a stable gel network and to hold the fibres together.

For proof of concept, a snowflake composite was prepared by assembling RICFP-prepreg segments. Owing to sticky surface of the prepregs, the snowflake form remained stable with 16 connecting points. The snowflake was successfully polymerised by RICFP, which can be seen in Fig. 14 and Video 2 (Supporting Information).

Conclusion

In this study, the radical polymerisation of 1,6-hexanediol diacrylate (HDDA) in presence of the frontally polymerisable components was investigated to form the B-stage for preparation of RICFP-prepreg. The study revealed that bis(*tert*-butylcyclohexyl)peroxydicarbonate (BCPC) was the most suitable radical thermal initiator which resulted in a fast polymerisation even at temperatures below 70 °C. Furthermore, in a formulation consisting of acrylates and epoxy monomers, radicals cleaved from BCPC selectively attacked the double bonds for the radical polymerisation and had no effect on the cationic ring-opening reaction. The study also indicated that with increase of HDDA amount the radical polymerisation was faster, while RICFP of the gels had lower frontal temperature and frontal velocity. Due to an increase in crosslink density, the higher HDDA amount led to a stiffer gel. With 10 wt% HDDA-based formulation, the resultant gel was sticky, bubble-free, flexible and especially had good storage stability. After 4 months at 50 °C, the epoxy group conversion just increased to 8% and a stable front was still obtained. The RICFP-prepreg was prepared with different weight percentages of carbon fibre tow. With up to 40 wt% fibres, RICFP was still possible and even faster frontal velocity than those of the matrix gel were obtained. The successful production of a snowflake composite was a first proof for the use of the RICFP-prepreg.

Experimental

Bisphenol-A diglycidylether (BADGE, Araldite MY 790-1, Huntsman), (3-ethyloxetan-3-yl)methanol (EOM, Doublemer 401, Double Bond Chemical), 1,1,2,2-tetraphenylethane-1,2-diol (TPED, Fluka), bis(4-*tert*-butylphenyl)-iodonium tetrakis(perfluoro-*tert*-butyloxy)aluminate (I-Al, Synthon), *α,α'*-azoisobutylronitrile (AIBN, Sigma-Aldrich), 4,4′-azobis(4-cyanovaleric acid) (ACVA, Sigma-Aldrich), potassium peroxodisulfate (KPS, Sigmal-Aldrich), bis(*tert*-butylcyclohexyl)peroxydicarbonate (BCPC, Sigma-Aldrich), ditetradecyl peroxydicarbonate (PODIC, Pergan), 1,6-hexanediol diacrylate (HDDA, abcr), carbon fibre tow (Toolcraft Conrad Electronic SE) were used as received.

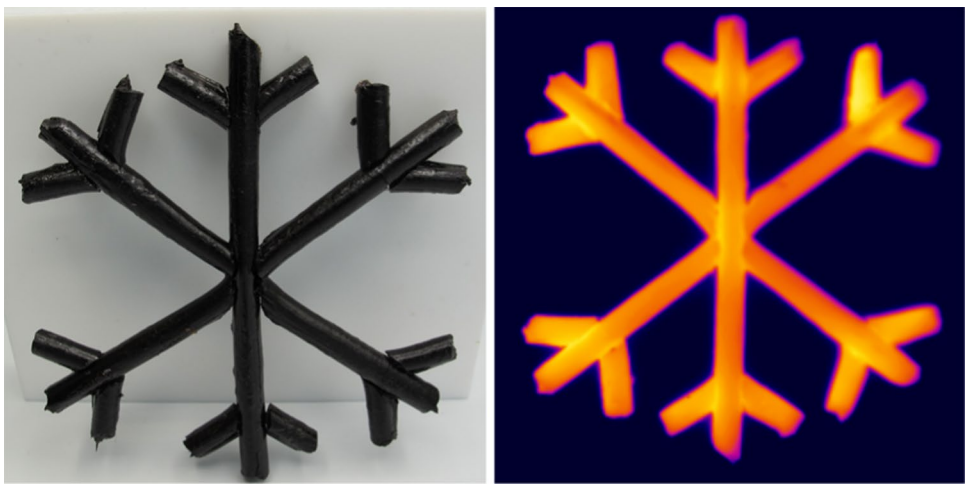

Fig. 14 The resultant snowflake composite cured by RICFP (left: digital image; right: IR image)

Preparation of formulations, gels and RICFP polymers

Radically polymerisable formulations were prepared with 1,6-hexanediol diacrylate and 2 mol% of different radical thermal initiators, called *HDDA-AIBN*, *HDDA-ACVA*, *HDDA-BCPC*, *HDDA-PODIC* and *HDDA-KPS* (Table S1, Supporting information). The formulations were homogenised using a vortex mixer for about 5 min.

A frontal formulation (called *FP*) was prepared with BADGE and EOM (with a molar ratio of 100:40, respectively), 2 mol% TPED as radical thermal initiator and 1 mol% I-Al as photoacid generator. The formulation was homogeneously mixed in a speed mixer (DAC 600.2 VAC-P, FlackTek Inc; 2350 rpm, 9 min).

Formulations for preparation of the gel were prepared as mixtures of *HDDA-BCPC* and *FP* with different ratios of 5:95, 10:90, 15:85 and 20:80 in wt%, respectively (Table S2, Supporting information). Then, the formulation was homogenised using the vortex mixer for 1 min. Afterwards, the formulation was purged with argon for 5 min and then treated in an ultrasound bath (with cool water) for 10 min to remove dissolved oxygen and bubbles. The obtained formulation was then transferred into a 1 cm^3 syringe and radically polymerised or gelled in a water bath at 60 °C, for 90 min (Fig. S1, Supporting information).

For comparison, two formulations were also treated with the same gelation condition, at 60 °C for 90 min. The first formulation is the frontal formulation (*FP*), while the second is a mixture of the frontal formulation and 0.88 wt% of BCPC. The value of 0.88 wt% is the weight percentage of BCPC compared to the weight of the frontal formulation portion in the formulation *FP_20HDDA-BCPC* (Table S2, Supporting information).

The treated formulations and the gels were then filled in a PTFE mold ($5 \times 5 \times 70$ mm^3) and polymerised by RICFP [32]. To follow the front position, a ruler was placed on the mold, along the specimen. During the reaction, a video was recorded using a camera and frontal temperatures were measured using an infrared camera (Optris Xi400). The initiation of RICFP was done on one end of the mold with UV/Vis-light of 320–500 nm and a light intensity of 3 W cm^{-2} at the tip of the light guide (about 500 mW cm^{-2} on surface of the specimen). After the initiation, the reaction propagated without further irradiation being necessary. The epoxy group conversion of the RICFP was determined by FT-MIR method which was discribed in our previous works [28, 33].

Differential scanning calorimetry measurement (DSC)

DSC measurement was conducted for the formulations consisting of HDDA and 2 mol% of different radical thermal initiators (AIBN, ACVA, BCPC, PODIC, KPS). 15 mg of each formulation were exactly weighed in an aluminium pan, which was subsequently sealed with an aluminium lid. An empty pan was used as reference for all measurements in this study. The pans were placed in a simultaneous thermal analyser (STA 449 F1 Jupiter, NETZSCH) and the temperature was risen from 25 to 200 °C with a heating rate of 5 °C min^{-1}. For analysis of the DSC plots, the onset of the exothermal peak was evaluated by laying tangents and intersecting them. Heat of the reaction was determined through the integration of heat flow over the exothermal peak.

To observe the radical polymerisation and cationic ring-opening reaction in one measurement, the DSC measurement was performed for the four formulations *FP*, *FP_BCPC*, *FP_20HDDA* and *FP_20HDDA-BCPC*. The measurement was done with the same above procedure, but with a lower heating rate of 1 °C min^{-1}.

Real time (RT)-NIR rheology measurement

To follow the gelation process of the formulation, RT-NIR rheology measurement was performed [43]. The measurements were done on a rheometer Anton Paar MCR302 WESP coupled with Bruker Vertex 80 FT-IR spectrometer. The rheometer was equipped with a parallel plate steel measuring system PP25 (plate diameter of 25 mm). Bottom plate of the rheometer was made by an optical glass which allows IR beam goes through. For protection of the glass plate, adhesive polyethylene tape (4668 MDPE, TESA) was used. A sample volume of 150 mm^3 was added on the center of the bottom glass plate, on the polyethylene tape. The rheology measurements were performed at 70 °C and a sample thickness (or gap size) of 200 µm. The formulation was sheared with a frequency of 1 Hz and a strain of 1% for at least 60 min. During the measurements, storage and loss moduli of the specimen were followed. There are some important values for observation of the radical polymerisation and properties of the gel. A point where the storage modulus starts to increase, t_s (min), which relates to the start of the radical polymerisation of HDDA. A point where the storage modulus crossovers the loss modulus, is defined as gel time, t_{gel} (min). In addition, the storage modulus value at 60 min of the specimen was collected to compare stiffness of the gels.

During the rheology measurement, the NIR spectra were also measured using a Bruker Vertex 80 FT-IR spectrometer with CaF_2 window. Every 3 min, a NIR spectrum was recorded in a wave number range of 4000–7000 cm^{-1} and a resolution of 8 cm^{-1}. In NIR spectra, peaks at 4530 and 4620 cm^{-1} are the epoxy and phenyl signals [43, 44]. The peaks at 4483, 4740 and 6160 cm^{-1} are assigned to the double bonds of HDDA [43, 45, 46]. Double bond and epoxy group conversion were calculated using the phenyl signal as a reference by equations below:

$$\text{Epoxy group conversion (EGC), \%} = \left(1 - \frac{\frac{A_{4530,t}}{A_{4620,t}}}{\frac{A_{4530,0}}{A_{4620,0}}}\right) \times 100\% \quad (1)$$

$$\text{Double bond conversion (DBC), \%} = \left(1 - \frac{\frac{A_{6160,t}}{A_{4620,t}}}{\frac{A_{6160,0}}{A_{4620,0}}}\right) \times 100\% \quad (2)$$

Here, $A_{4530,_0}$ and $A_{4530,_t}$ are integral of the epoxy signal (4530 cm^{-1}) at 0 and t min of the measuring time, respectively. $A_{4620,_0}$ and $A_{4620,_t}$ are integral of the reference (4620 cm^{-1}) at 0 and t min of the measuring time, respectively. $A_{6160,_0}$ and $A_{6160,_t}$ are integral of the double bond signal (6160 cm^{-1}) at 0 and t min of the measuring time, respectively.

Due to the overlap of the epoxy (4530 cm^{-1}) and the double bond signal (4483 cm^{-1}), separation of these signals was done using a peak deconvolution function in OriginPro 2020 SR1 9.7.0.188. After the deconvolution was done, the signal area of the peaks (4530, 4620 and 6160 cm^{-1}) were integrated to calculate the above conversion. A procedure of the peak deconvolution was described in the supporting information.

Determination of gel content and light microscope images

Gel content of the specimens (*FP_5HDDA-BCPC*, *FP_10HDDA-BCPC*, *FP_15HDDA-BCPC* and *FP_20HDDA-BCPC*) was determined using dichloromethane as a solvent for extraction. A thin section of approximate 1 mm thickness and 4.8 mm diameter (about 20 mg) was immersed in 0.5 cm^3 dichloromethane in a 2 cm^3 brown vial. Every 1 h the old solvent was collected and replaced by the same new amount. After 2 h, the solvent was exchanged one more time and then the vial was kept overnight. Afterwards, the gel was washed 3 times with a small amount of solvent before dried in a vacuum oven (at 50 °C, 5 mbar) for at least 24 h. The gel content was calculated following a formula:

$$\text{Gel content (\%)} = \frac{m_1}{m_0} \times 100\% \quad (3)$$

Here, m_0 and m_1(mg) are weight of a thin section before and after extracted with dichloromethane, respectively.

The experiment was done triplicates and results were averaged. From the collected solution of the gel consisting of 10 wt% HDDA the solvent was removed using a rotary evaporator at 25 °C. Then, residues in the vial were dissolved in acetonitrile and characterised by high performance liquid chromatography (HPLC).

For light microscopic observation, a thin section of about 0.5 mm thickness was cut from the gel consisting of 10 wt% HDDA portion. The section was put on a petri dish which was placed under a light microscope (ZEISS AX10). To observe the extraction, dichloromethane was added to the petri dish. The whole experiment was recorded using a digital camera (Canon Powershot G12) which was connected to the light microscope. To observe swelling process, similar process was also done with a dried specimen from the gel content experiment.

Storage stability test of the formulation and the gel

To study pot-life of the gel formulations, an amount of *FP_10HDDA-BCPC* and *FP_20HDDA-BCPC* was collected right after preparation and stored at room temperature. Following a storage time, viscosity and NIR spectra of the formulations were measured. The viscosity measurement was done on a rheometer (Anton Paar MCR302 WESP) equipped with a PP25 measuring system. The measurement was conducted in rotation with a shear rate of 100 s^{-1} for the duration of 100 s at a constant temperature of 25 °C. For the analysis, the last viscosity value of this 100 s period was taken. All measurements were conducted in duplicates and the results were averaged. During the viscosity measurement, a NIR spectra of the formulation was recorded using Bruker Vertex 80 FT-IR spectrometer, in a range of 4000–7000 cm^{-1}, a resolution of 8 cm^{-1} and 16 scans. The double bond and epoxy group conversion were calculated following the above equations Eqs. (1) and (2).

To study storage stability, the gel was stored in an oven at 50 °C. Following a storage time, the NIR spectra were recorded for the gel at 25 °C. The epoxy group conversion was calculated following the above equation Eq. (1) to investigate the storage stability of the gel. RICFP was also carried out for the stored gels. The frontal parameters were measured and compared with those values of the fresh gel on day zero.

Dynamic mechanical thermal analysis (DMTA)

DMTA measurement was conducted for all above RICFP specimens. A cylinder specimen (diameter of about 4.6 mm) obtaining from the above RICFP was cutoff irradiation part and polished to have a length of about 40 mm. Then, this 40-mm long cylinder was polished both sides to have a symmetry shape with around 3 mm in thickness. The final specimen for DMTA was 40 mm long, 3 mm thick and 4.6 mm wide (Fig. S2, Supporting information). The measurement was done in torsion deformation, at an initial strain of 0.1% and a frequency of 1 Hz. Two heating cycles were conducted for all measurements in a temperature range from − 50 to

200 °C and a heating rate of 2 °C min^{-1}. The glass transition temperature (T_g) was defined as peak of the tan δ curve.

Preparation of RICFP-prepreg and its composites

The formulation (*FP_10HDDA-BCPC*) consisting of 10 wt% of *HDDA-BCPC* and 90 wt% of *FP* was used for this study. RICFP-prepregs were prepared in a glass tube with an inner diameter of 6 mm and a length of 200 mm. Carbon fibre tow was exactly weighed and inserted into the glass tube. Then, the formulation was transferred into the tube to impregnate the fibres using a syringe. Afterwards, the tube was closed at both sides and the formulation was gelled at 60 °C, for 90 min. Resultant RICFP-prepreg was collected by applying pressure air at one end of the tube. The procedure for preparation of the prepreg is illustrated in Fig. S3 (Supporting information). Fibre content was calculated as wt% by division of fibre weight to total weight of the prepreg.

For proof of concept, a composite with snowflake form was produced using RICFP-prepregs. The prepreg was cut to many segments with different lengths. Then, the segments were assembled together by hands. Owing to sticky surface, the snowflake form was remained (Fig. S4, Supporting information). There were 16 connecting points in the snowflake structure. The frontal polymerisation was initiated at the centre of the specimen using an UV light. The polymerisation process was recorded using a digital and an IR camera.

Acknowledgements We would like to thank the OeAD, the Ernst Mach Grant Asea-Uninet (funded by Bundesministerium für Wissenschaft, Forschung und Wirtschaft, No. ICM-2017-06830) and the Chemical Monthly Fellowship (funded by Österreichischen Akademie der Wissenschaften, No. 64870) for supporting this study.

Funding Open Access funding provided by TU Wien (TUW).

Open Access This article is licensed under a Creative Commons Attribution 4.0 International License, which permits use, sharing, adaptation, distribution and reproduction in any medium or format, as long as you give appropriate credit to the original author(s) and the source, provide a link to the Creative Commons licence, and indicate if changes were made. The images or other third party material in this article are included in the article's Creative Commons licence, unless indicated otherwise in a credit line to the material. If material is not included in the article's Creative Commons licence and your intended use is not permitted by statutory regulation or exceeds the permitted use, you will need to obtain permission directly from the copyright holder. To view a copy of this licence, visit http://creativecommons.org/licenses/by/4.0/.

References

1. Pansart S (2013) 6—prepreg processing of advanced fibre-reinforced polymer (FRP) composites. In: Bai J (ed) Advanced fibre-reinforced polymer (FRP) composites for structural applications. Woodhead Publishing, Philadelphia, p 125
2. Hamerton I, Mooring L (2012) 7—the use of thermosets in aerospace applications. In: Guo Q (ed) Thermosets. Woodhead Publishing, Philadelphia, p 189
3. Ellis B (1993) Chemistry and technology of epoxy resins, 1st edn. Blackie Academic & Professional, London
4. Pham HQ, Marks MJ (2004) Epoxy resins. Ullmann's encyclopedia of polymer science and technology. Wiley, Weinheim, p 1643
5. Stewart R (2012) Reinf Plast 56:18
6. Brøndsted P, Lilholt H, Lystrup A (2005) Annu Rev Mater Res 35:505
7. Javaid U, Ling C, Cardiff P (2020) Eng Fail Anal 116:104730
8. Prince K (2002) Reinf Plast 46:48
9. Composite developments drive auto industry forward (2014). Reinf Plast, p 22. https://doi.org/10.1016/S0034-3617(14)70135-3
10. Centea T, Grunenfelder LK, Nutt SR (2015) Compos A 70:132
11. Stewart AL, Poursartip A (2018) Compos A 112:239
12. Gopal KVN (2016) 14—product design for advanced composite materials in aerospace engineering. In: Rana S, Fangueiro R (eds) Advanced composite materials for aerospace engineering. Woodhead Publishing, Philadelphia, p 413
13. Fawaz Z (2016) 15—Quality control and testing methods for advanced composite materials in aerospace engineering. In: Rana S, Fangueiro R (eds) Advanced composite materials for aerospace engineering. Woodhead Publishing, Philadelphia, p 429
14. Pouladvand AR, Mortezaei M, Fattahi H, Amraei IA (2020) Compos A 132:105852
15. Ahn KJ, Peterson L, Seferis JC, Nowacki D, Zachmann HG (1992) J Appl Polym Sci 45:399
16. Hagnauer GL, Dunn DA (1981) J Appl Polym Sci 26:1837
17. Hayaty M, Honarkar H, Beheshty MH (2013) Iran Polym J 22:591
18. Fedtke M, Domaratius F, Pfitzmann A (1990) Polym Bull 23:381
19. Morgan RJ, Walkup CM, Hoheisel TH (1985) J Appl Polym Sci 30:289
20. George GA, Cash GA, Rintoul L (1996) Polym Int 41:169
21. Pojman JA (2012) 4.38—frontal polymerisation. In: Matyjaszewski K, Möller M (eds) Polymer science: a comprehensive reference. Elsevier, Amsterdam, p 957
22. Fiori S, Mariani A, Ricco L, Russo S (2003) Macromolecules 36:2674
23. Mariani A, Fiori S, Chekanov Y, Pojman JA (2001) Macromolecules 34:6539
24. Nason C, Roper T, Hoyle C, Pojman JA (2005) Macromolecules 38:5506
25. Uflyand IE, Zhinzhilo VA, Dzhardimalieva GI (2019) ChemistrySelect 4:2105
26. Ebner C, Mitterer J, Eigruber P, Stieger S, Riess G, Kern W (2020) Polymers 12:1291
27. Mariani A, Bidali S, Fiori S, Sangermano M, Malucelli G, Bongiovanni R, Priola A (2004) J Polym Sci Pol Chem 42:2066
28. Tran AD, Koch T, Knaack P, Liska R (2020) Compos Part A 132:105855. https://doi.org/10.1016/j.compositesa.2020.105855
29. Sangermano M, Antonazzo I, Sisca L, Carello M (2019) Polym Int 68:1662
30. Sangermano M, D'Anna A, Marro C, Klikovits N, Liska R (2018) Compos B 143:168
31. Bomze D, Knaack P, Koch T, Jin HF, Liska R (2016) J Polym Sci Pol Chem 54:3751
32. Bomze D, Knaack P, Liska R (2015) Polym Chem 6:8161
33. Knaack P, Klikovits N, Tran AD, Bomze D, Liska R (2019) J Polym Sci Pol Chem 57:1155
34. Klikovits N, Liska R, D'Anna A, Sangermano M (2017) Macromol Chem Phys 218:1700313
35. Kaur M, Srivastava AK (2002) J Macromol Sci Polym Rev 42:481
36. Nesvadba P (2012) Radical polymerisation in industry. In: Studer A (ed) Encyclopedia of radicals in chemistry, biology and materials. Major Reference Works. Wiley, New Jersey, p 1701

37. Danso R, Hoedebecke B, Whang K, Sarrami S, Johnston A, Flipse S, Wong N, Rawls HR (2018) Dent Mater 34:1459
38. Fouassier JP, Lalevée J (2014) Polymers 6:2588
39. Nowers JR, Narasimhan B (2006) Polymer 47:1108
40. Decker C, Viet TNT, Decker D, Weber-Koehl E (2001) Polymer 42:5531
41. Polymerisation of monomers with organic peroxides. The Peroxide Company-PERGAN. https://www.pergan.com/files/downloads/Polymerization_HP_EN.pdf. Accessed 14 Nov 2020
42. Applications: Free Radical Initiators. Sigma Aldrich. https://www.sigmaaldrich.com/content/dam/sigma-aldrich/docs/Aldrich/General_Information/thermal_initiators.pdf. Accessed 14 Nov 2020
43. Gorsche C, Harikrishna R, Baudis S, Knaack P, Husar B, Laeuger J, Hoffmann H, Liska R (2017) Anal Chem 89:4958
44. Lachenal G, Pierre A, Poisson N (1996) Micron 27:329
45. Šašić S, Ozaki Y, Olinga A, Siesler HW (2002) Anal Chim Acta 452:265
46. Grabska J, Ishigaki M, Beć KB, Wójcik MJ, Ozaki Y (2017) J Phys Chem A 121:3437
47. Goli E, Robertson ID, Agarwal H, Pruitt EL, Grolman JM, Geubelle PH, Moore JS (2019) J Appl Polym Sci 136:47418
48. Robertson ID, Yourdkhani M, Centellas PJ, Aw JE, Ivanoff DG, Goli E, Lloyd EM, Dean LM, Sottos NR, Geubelle PH, Moore JS, White SR (2018) Nature 557:223

Publisher's Note Springer Nature remains neutral with regard to jurisdictional claims in published maps and institutional affiliations.